Journal of Applied Electrochemistry **32**: 795–803, 2002.

Microstructural and corrosion studies of Ti alloy (IMI 834) in acidic solutions

V.B. SINGH* and A. GUPTA
Department of Chemistry, Banaras Hindu University, Varanasi - 221005, India
*(*author for correspondence, e-mail: vijaybs@banaras.ernet.in)*

Received 8 January 2001; accepted in revised form 20 November 2001

Key words: heat treatment, microstructure, passivity, polarization, STM, titanium alloy

Abstract

The electrochemical polarization behaviour of a titanium alloy (IMI 834) was studied in different concentrations of aqueous and ethylene glycolic solutions of hydrochloric and phosphoric acid at 30 °C. The influence of furnace cooled (FC), air cooled (AC) and water quenched (WQ) heat treatments and microstructure on polarization behaviour was also studied. An active passive transition and a large range of passivity potential were observed in aqueous and glycolic solutions of the acids. The magnitudes of the critical current density (i_c) and passive current density (i_p) were higher for hydrochloric acid in comparison to phosphoric acid. Values of i_c and i_p were lower in ethylene glycol–hydrochloric acid up to 7 M and were higher above 7 M hydrochloric acid–ethylene glycol solutions as compared to the corresponding hydrochloric acid concentrations. However, these values were always lower in ethylene glycol–phosphoric acid than in phosphoric acid solutions. The microstructure of the alloy after solution treatment (1080 °C, 30 min; FC, AC and WQ) showed single phase transformed β structure. The increase in the cooling rate enhances the fineness of the β laths. The working electrode surface was examined by scanning electron microscopy (SEM) and scanning tunnelling microscopy (STM).

1. Introduction

Titanium and its alloys, owing to their biocompatibility, high corrosion resistance, light weight and various mechanical properties, are used extensively as artificial joints, bone plates and dental implants. Concentrated efforts over the last three decades has led to the development of excellent conventional titanium alloys [1] to enhance the lower limits of superalloy to 873 K.

Alloy IMI 834, employed in the present investigation, is a relatively new medium strength alloy developed for improved temperature and tensile/fatigue situations and has the highest maximum service temperature (600 °C ~ 1200 °C) among conventional commercial titanium alloys. Its major applications include compressor discs and blades for the aerospace gas turbine engine industry.

Substantial work related on the corrosion behaviour of titanium and its alloys in different aqueous and reducing acid solutions has been reported [2–7]. Passivated Ti exhibits poor corrosion resistance in concentrated reducing acids, such as HCl or H_2SO_4. Therefore, alloying additions that can promote the stability of the protective oxide film in a reducing acidic environment are desirable. Alloying elements, such as Nb and Zr, are strong oxide formers [8] and resist chemical dissolution in reducing acids [9–11]. The alloy under the present investigation also contains these elements. We have, therefore, chosen to undertake a study of its electrochemical corrosion behaviour in reducing acids (HCl, H_3PO_4) since these acids are in common commercial use. The corrosion behaviour of IMI 834 alloy in different concentrations of aqueous and ethylene glycolic solutions of hydrochloric and phosphoric acids has been investigated. The influence of various heat treatments on its corrosion behaviour has also been investigated.

2. Experimental details

The titanium alloy (IMI 834) was procured from M/S Imperial Metal Industries (UK). The alloy (IMI 834) with near α composition, contained 5.8 Al, 4 Sn, 3.5 Zr, 0.7 Nb, 0.5 Mo, 0.35 Si, 0.06 C (by wt %). The experimental setup, working procedure and specimen preparation are the same as described elsewhere [3–5, 12]. Polarization studies were performed potentiostatically (Wenking. POS73) in aerated solution under unstirred conditions. Prior to polarization measurements, the working electrode of 2 cm^2 exposed surface area was immersed in the experimental solution for about 30 min to attain a stable value of open circuit potential (OCP). Polarization was done by starting at a negative potential and moving in the positive direction, in different acid concentrations unless otherwise stated.

Acid solutions of different concentrations were prepared by diluting a stock solution of concentrated hydrochloric acid or phosphoric acid (AR grade) with double distilled water and ethylene glycol. All experiments were performed at 30 ± 1 °C unless otherwise mentioned. A saturated calomel electrode (SCE) was used as reference.

Solution treatments were given to the specimen in the β phase field at 1080 °C for 30 min under vacuum (10^{-3} torr) and the specimens were cooled in a furnace (FC), air (AC) and water (WQ). For solution treatments the polished samples were sealed in a silica tube along with titanium getter at 10^{-3} torr vacuum.

The working electrode surface was examined using scanning electron microscopy (Philips XL-20) and scanning tunnelling microscopy (Metris-2000 Burleigh).

3. Results and discussion

3.1. *Hydrochloric acid and ethylene glycolic–hydrochloric acid solutions*

The open circuit potential (o.c.p.) of the alloy in different concentrations of aqueous and ethylene glycolic solutions of hydrochloric and phosphoric acids ranged between −440 and −650 mV vs SCE and showed a tendency to move in the less noble direction with an increase in acid (HCl or H_3PO_4) concentration in aqueous or ethylene glycol solution.

Figure 1 represents the cathodic and anodic polarization curves of titanium alloy in different concentrations (3, 5, 7, 9 and 11 M) of aqueous hydrochloric acid, at 30 °C. The nature of the cathodic polarization curves for the alloy in different acid concentrations is similar and the current density increased as the potential moved negatively. The linear nature of the cathodic polarization curves indicated an activation controlled cathodic reaction. The cathodic reaction was hydrogen evolution and the Tafel slope values ranged between 55–125 mV decade^{-1}.

The alloy showed a distinct active–passive behaviour in the above concentration range (Figure 1). The critical current density (i_c) for passivity and the passive current density (i_p) increased substantially (from 84 to 2400 μA cm^{-2} and 8 to 96 μA cm^{-2}, respectively) with increase in hydrochloric acid concentration. The potential at which passivity started was the same for all concentrations. A wide and stable passive potential range was invariably observed. The Ti–6A1–4V alloy also showed similar anodic polarization curves in different hydrochloric acid concentrations [5]. However, i_c and i_p were always higher for Ti–6A1–4V than for IMI 834 alloy at different hydrochloric acid concentrations. Thus, IMI 834 alloy appears more corrosion resistant than Ti–6A1–4V. The dissolution of anodic Ti oxides, upon exposure to a reducing acid has been correlated with the conversion of TiO_2 to hydrated TiOOH or by direct chemical dissolution to TiO^{2+} or $Ti(OH)^{3+}$ [16, 17]. It is understood that the alloying additions Nb and Zr, which are strong candidates for formation of complex homogeneous oxyhydroxides, resist chemical dissolution in reducing acids [9–11] and likely form

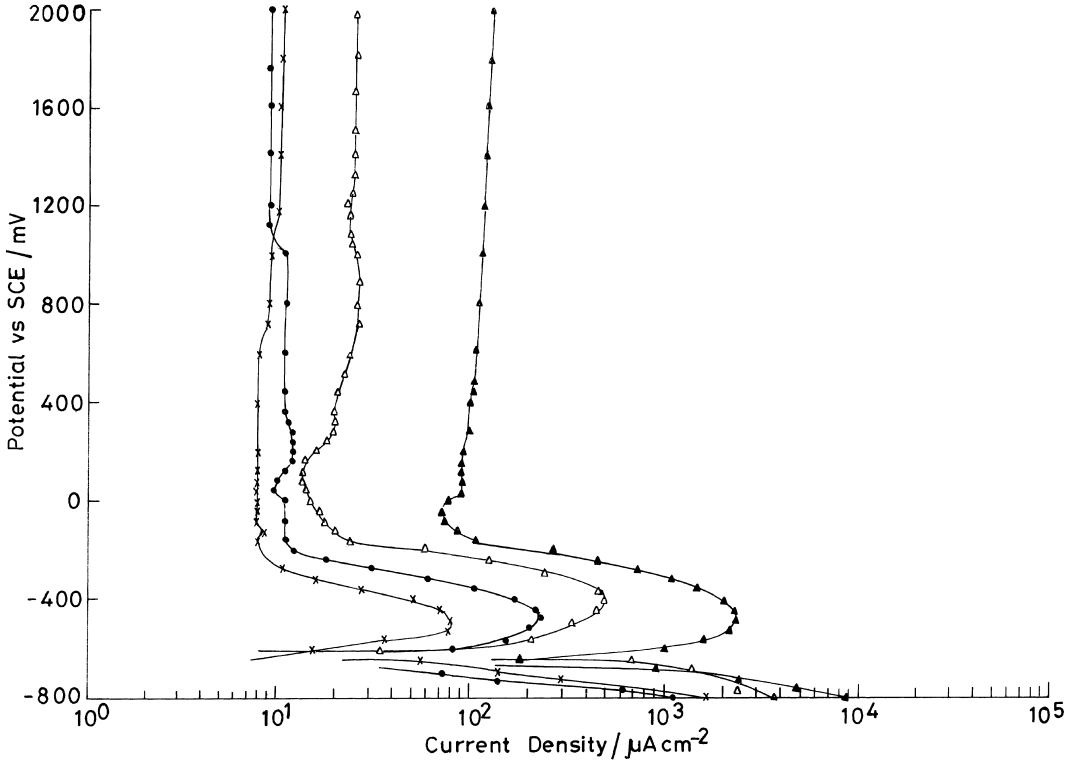

Fig. 1. Polarization curves of titanium alloy (IMI 834) in different concentrations of aqueous hydrochloric acid, at 30 °C: (–×–) 3 M, (–●–) 7 M, (–Δ–) 9 M and (–▲–) 11 M HCl.

M—O bonds of high strength [8]. Such resistance to oxide dissolution can be attributed to the formation of a mixed Ti–Zr oxide in the form of a double oxyhydroxide that is thermodynamically stable at low pH and potential [18, 19]. Similar anodic polarization curves have also been observed by others [5, 13–15] for titanium in different hydrochloric acid concentrations.

Hydrogen evolution was seen during the cathodic polarization; there is likelihood of formation of hydride on the surface [20, 21]. Several authors [22] have noted that a hydride layer forms and that its thickness diminishes as the anodic potential [23] increases. The presence of hydride was inferred here and this compound may intervene in the formation of tetravalent species in the solution [24]. Above a certain critical concentration, Ti(IV) ions in solution passivate [24] an active surface or inhibit the anodic dissolution of titanium [25]. That the intervened Ti (IV) formation is not effectively inhibiting may be due to a certain critical concentration requirement and resulting in higher passivity current (i_p) particularly in concentrated solution ($\geqslant$7 M) (Figure 1). The acidity may also be responsible for such behaviour. Titanium dissolves producing Ti(III) ions in the active potential region and Ti(IV) ions in the passive potential region [26, 27]. The passivation was considered mainly to be due to the slightly soluble tetravalent adsorbed species and the passivity finally observed can be ascribed to the formation of a very slightly soluble oxide layer (TiO_2) in hydrochloric acid. Oxide destabilization can occur by chemical dissolution of the oxide in a reducing acid and spatially localized oxide film breakdown due to the ingress of anionic species such as chlorides (Cl^-) and bromides (Br^-), particularly at Al or Si-rich inclusions [28].

The cathodic and anodic polarization behaviours of IMI 834 alloy in different concentrations of hydrochloric acid in ethylene glycol (Figure 2, at 30 °C) showed that, on increasing the hydrochloric acid concentration in ethylene glycol, the cathodic polarization curves shifted towards a higher current density region and closely resembled those observed in different concentrations of aqueous hydrochloric acid (Figure 1); thus the cathodic reaction was hydrogen evolution. The cathodic Tafel slope values ranged between 68–135 mV $(decade)^{-1}$.

Active–passive behaviour was observed for the alloy in different concentrations of hydrochloric acid in ethylene glycol (Figure 2). The alloy became passive in the negative potential region. On comparing the anodic polarization behaviour of the alloy in different concentrations of aqueous and glycolic solutions of HCl (Figures 1 and 2) it was observed that the curves followed a similar trend with increase in hydrochloric acid concentration either in aqueous or ethylene glycol solutions. However, the values of i_c and i_p were considerably lower in glycolic solution in comparison to aqueous solutions (3–7 M HCl). But at higher acid concentration (8–10 M) the values of i_c and i_p were higher in the glycolic solutions (Figure 2) corresponding to those in aqueous solution. The acidic glycolic solutions may thus be classified into two groups ethylene glycol rich solution (3–7 M HCl) and hydrochloric acid rich solution (>7 M HCl). The low values of i_c and i_p in

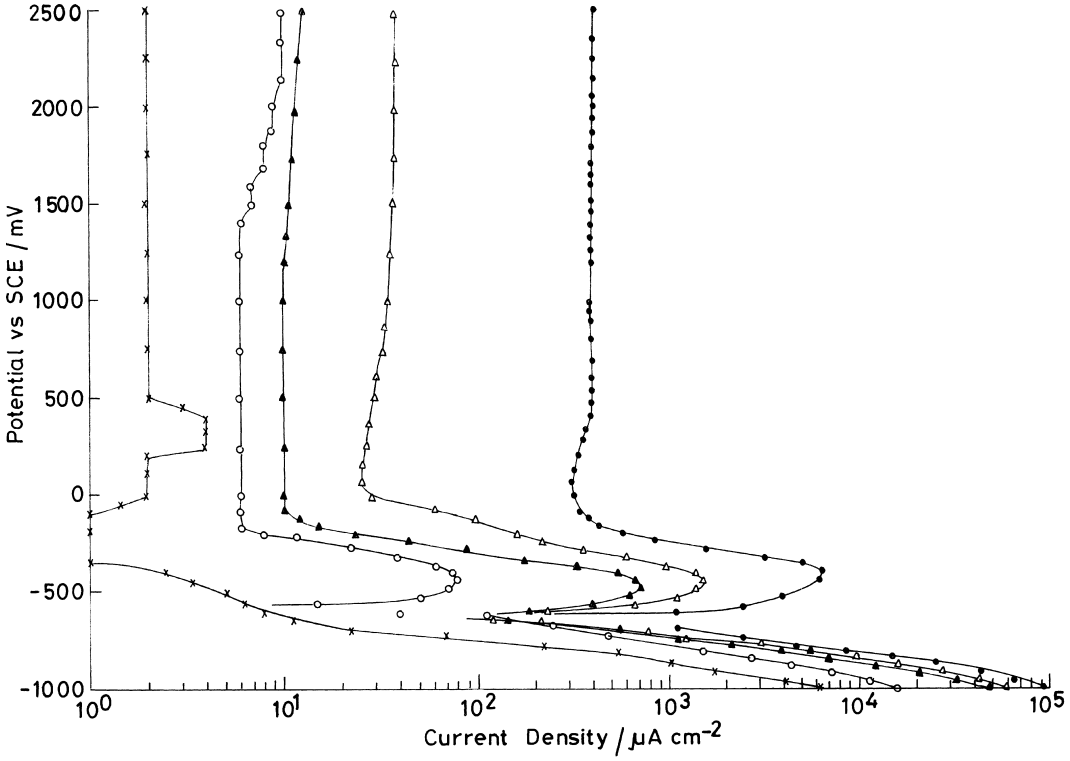

Fig. 2. Polarization curves of titanium alloy (IMI 834) in different concentrations of hydrochloric acid in ethylene glycol solution, at 30 °C: (–×–) 5, (–O–) 7, (–▲–) 8, (–Δ–) 9 and (–●–) 10 M HCl.

glycolic solution at the corresponding aqueous hydrochloric acid concentration may be due to the relatively lower dielectric constant of ethylene glycol. However, in acid rich solution the higher value of i_c and i_p can be ascribed to a high dielectric constant of the resulting solution, and since ethylene glycol behaves as an acid compared to water, the corrosiveness of the solution towards the alloy increased at higher hydrochloric acid concentration (> 7 M HCl) in ethylene glycol.

3.2. *Phosphoric acid and ethylene glycolic phosphoric acid solutions*

The cathodic and anodic polarization behaviour of the titanium alloy in different phosphoric acid concentrations (3.24, 7.28, 10.92 and 13 M) are illustrated in Figure 3, at 30 °C. Hydrogen evolution took place during the cathodic polarization at all acid concentrations and the Tafel values ranged between 77 and 135 mV (decade)$^{-1}$.

Active–passive behaviour was exhibited at all phosphoric acid concentrations (Figure 3). The critical current density (i_c) increased (from 5.4 to 69 μA cm^{-2}) with increase in concentration. An increase in i_p was found up to 7.28 M and thereafter it decreased to the lowest value of 1.86 μA cm^{-2} at the highest concentration. In dilute solution the increase in i_c was greater than that at the higher concentration. Such a change in the corrosiveness of the acid towards the alloy may be due to changes in the structure of the acid solution with dilution. In highly concentrated phosphoric acid the phosphate ions are interconnected by hydrogen bonds, but in dilute solution, these ions are hydrogen bonded to the water liquid lattice rather than to other phosphate ions [29]. Therefore, it is expected that a dilute solution of phosphoric acid has a lower solvation effect as compared to a concentrated one.

An oxide type film formation is most likely on the alloy surface with a small difference in their protective properties [30]. The oxide is typically TiO_2 but may consist of mixtures of other titanium oxides including TiO_2, Ti_2O_3 and TiO. The current densities in different regions were always higher in aqueous hydrochloric acid than phosphoric acid solutions (Figures 1 and 3), which can be attributed to the greater aggressiveness of hydrochloric acid than that of phosphoric acid. This is partly because of the many fold higher dielectric constant of hydrochloric acid compared to phosphoric acid.

Figure 4 represents the cathodic and anodic polarization behaviours of the alloy in phosphoric acid–ethylene glycol solutions. The cathodic reaction in each case was hydrogen evolution and the Tafel slope values ranged between 80 and 150 mV (decade)$^{-1}$. The anodic polarization curves revealed active–passive behaviour and, on increasing the phosphoric acid concentration (3.24 to 10.9 M) in ethylene glycol, the curves shifted towards the higher current density region.

The anodic polarization curves always shifted towards lower current density at each concentration in the glycolic solution in comparison to aqueous phosphoric acid (Figures 3 and 4). The i_c and i_p values were lower in acidic glycolic solution than in aqueous phosphoric acid.

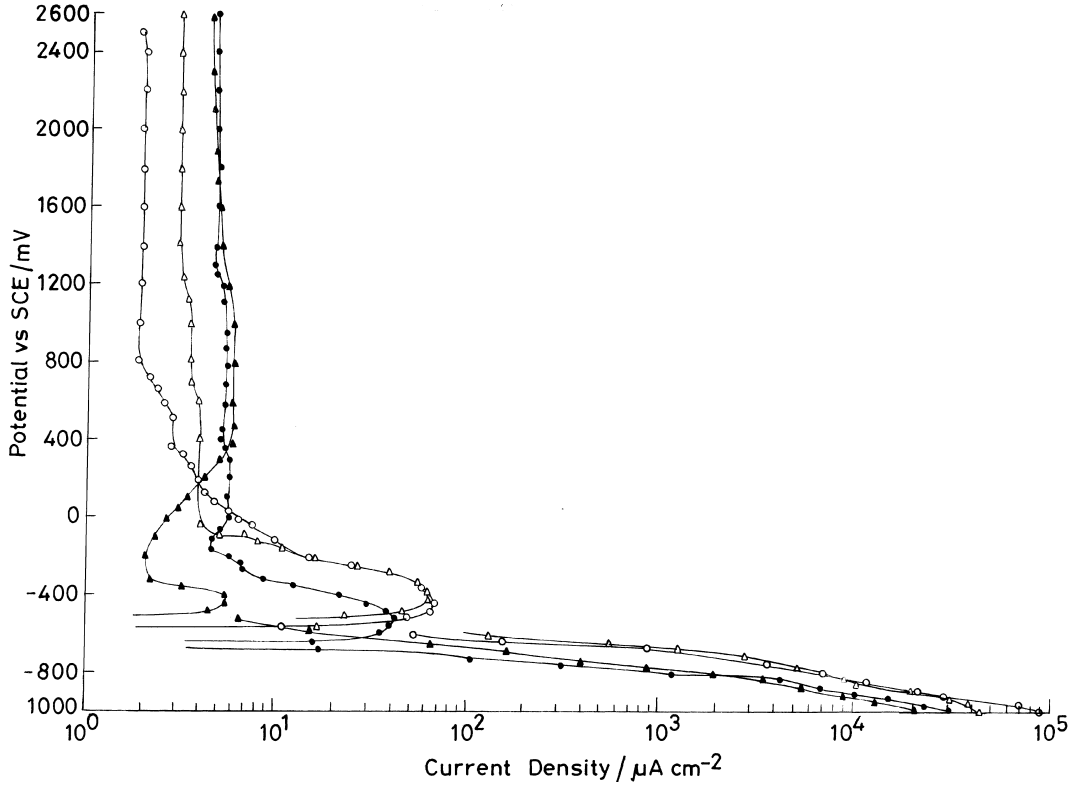

Fig. 3. Polarization curves of titanium alloy (IMI 834) in different concentrations of aqueous phosphoric acid, at 30 °C: (–▲–) 3.24, (–●–) 7.28, (–Δ–) 10.92 and (–O–) 13.0 M H_3PO_4.

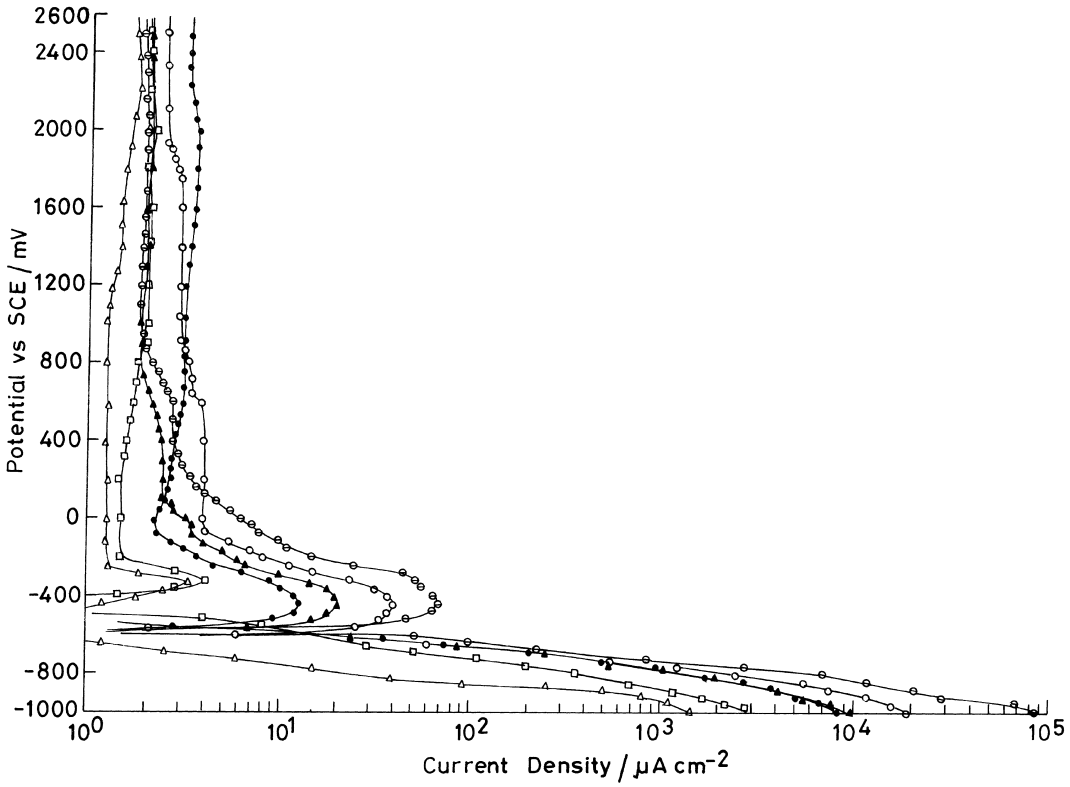

Fig. 4. Polarization curves of titanium alloy (IMI 834) in different concentrations of phosphoric acid in ethylene glycol solution, at 30° C: (–Δ–) 3.64, (–□–) 5.0, (–●–) 7.28, (–▲–) 9.0, (–○–) 10.9 and (-⊖⊖) 13.0 M H_3PO_4.

As water is replaced by ethylene glycol in solution there is an increase in viscosity with increasing ethylene glycol concentration in the solution mixture. Consequently a decrease in i_c showed that in glycolic solution viscosity plays a predominant role in the dissolution process.

3.3. *Influence of heat treatment*

Figure 5 represents the cathodic and anodic polarization behaviours of FC, AC, WQ and as received specimen of titanium alloy in aqueous 7 M hydrochloric acid and 10 M hydrochloric acid in ethylene glycol solution. The cathodic polarization curves for the FC, AC and WQ specimens shifted towards the higher current density region as compared to that of the as received specimen in aqueous 7 M hydrochloric acid. However, in 10 M HCl–ethylene glycol solution the cathodic curves shifted towards the higher current density region for AC and WQ specimens compared to those for the as received specimen. In both the media, the nature of the curves was similar in all cases, except for variation of current density.

The anodic polarization curves for FC, AC and WQ specimens showed active–passive behaviour in 7 M hydrochloric acid and these curves shifted towards higher current density in comparison to the as received specimen. The maximum value of i_c was observed for the AC specimen followed by the WQ and FC specimens. A slightly lower corrosion resistance observed for the alloy as compared to the various heat treated specimens may be attributed to the multiphase microstructure of the specimen after heat treatment. It is probable that the alloying elements produce a significant potential difference between the α and β phases causing a relatively high dissolution current, which increases as the ratio of the amounts of α and β phases increases [31]. The dissolution may be accelerated by the galvanic effects and the unfavourable area ratio (large α cathodic area and small β anodic area).

Active–passive behaviour was also observed for the FC, AC and WQ specimens in 10 M hydrochloric acid in ethylene glycol, where the curves shifted towards the lower current density region for the FC, AC and WQ specimens as compared to those of as received specimen.

The cathodic and anodic polarization behaviours of the FC, AC, WQ and as received specimens in 13 M phosphoric acid are illustrated in Figure 6. The cathodic polarization curves resembled that of the as received specimen and the cathodic reaction was hydrogen evolution.

The anodic polarization curves (Figure 6) showed active–passive behaviour for the specimen with various microstructures in 13 M phosphoric acid. The value of i_c was slightly higher for as received than for various heat treated specimens. The variation in the values of i_c and i_p for various heat treated specimens are due to their different microstructures and the difference in the electrochemical behaviour may be due, in part, to the difference in their crystal structure [32].

Figure 7 represents the cathodic and anodic polarization behaviours of the FC, AC, WQ and as received

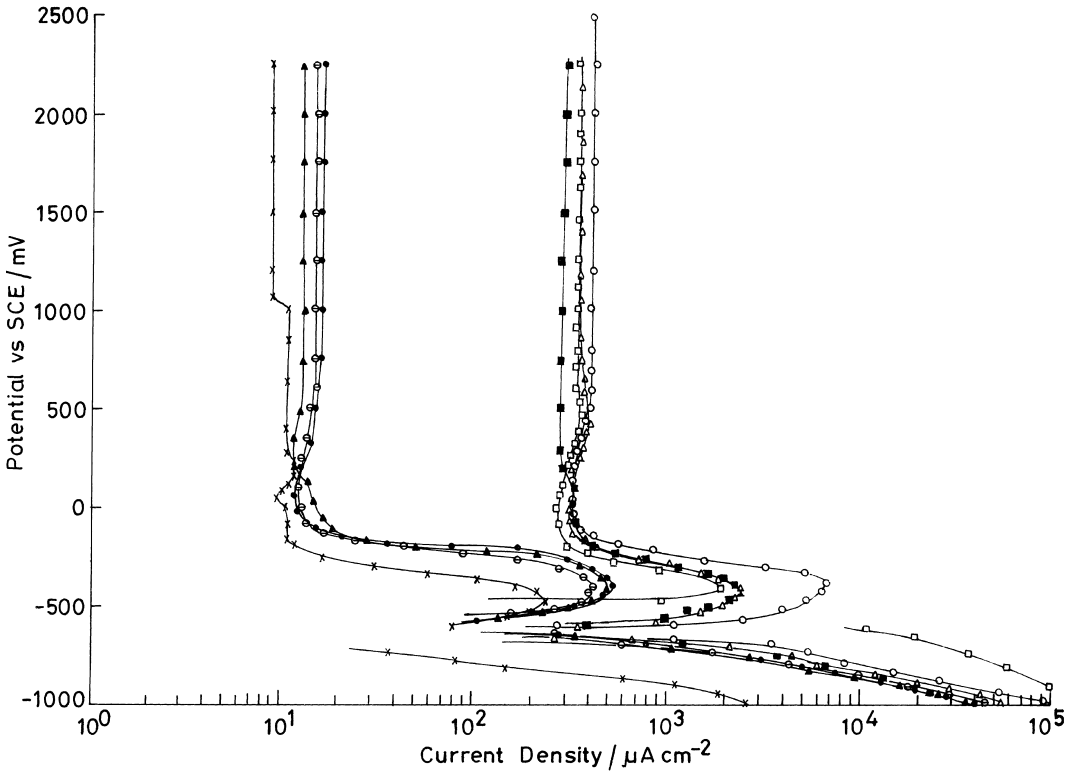

Fig. 5. Polarization curves of titanium alloy (IMI 834) in aqueous 7 M HCl and 10 M hydrochloric acid in ethylene glycol solution, at 30 °C (after heat treatment). 7 M HCl: (–O–) FC, (–●–) AC, (–▲–) WQ and (–×–) as received. 10 M HCl + EG: (–□–) FC, (–■–) AC, (–△–) WQ and (–O–) as received.

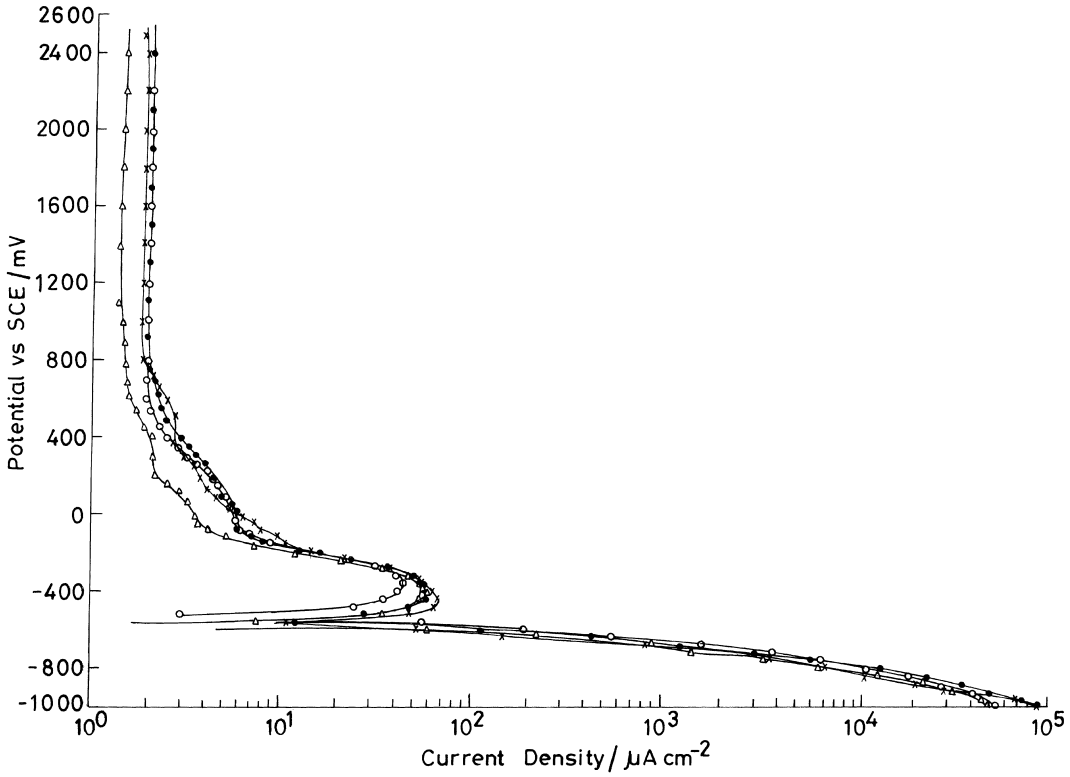

Fig. 6. Polarization curves of titanium alloy (IMI 834) in 13 M phosphoric acid, at 30 °C (after heat treatment): Key: (–O–) FC, (–●–) AC, (–△–) WQ and (–×–) as received.

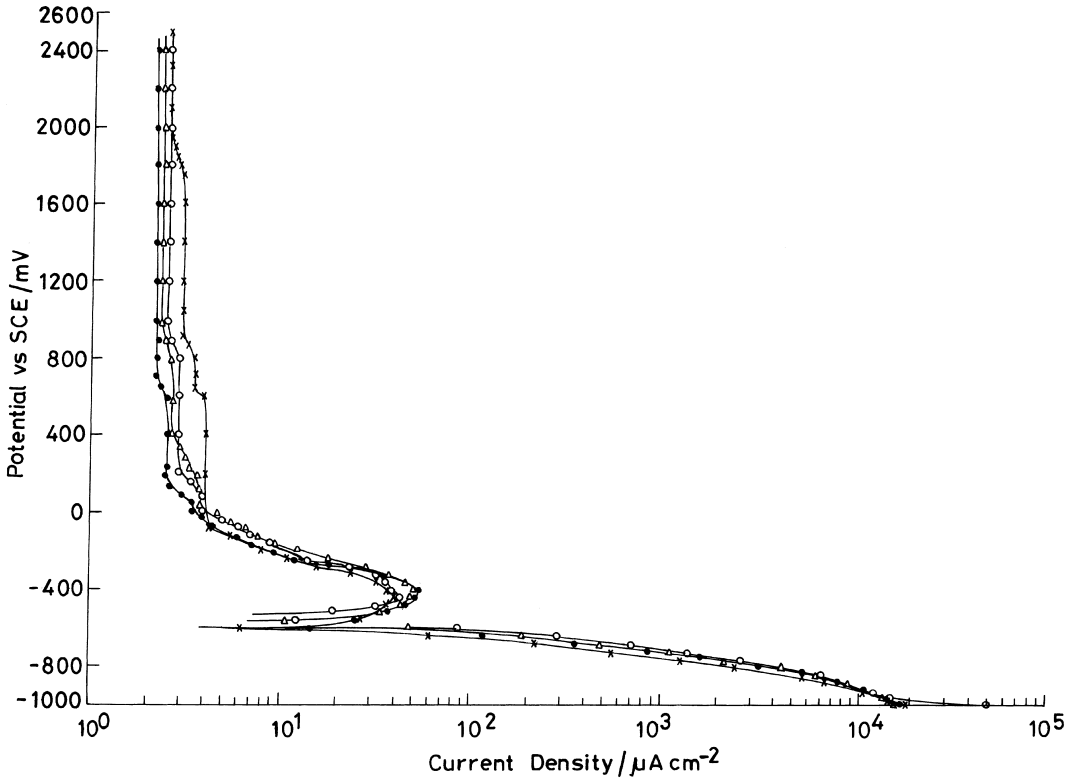

Fig. 7. Polarization curves of titanium alloy (IMI 834) in 10.92 M phosphoric acid in ethylene glycol, at 30 °C (after heat treatment). Key: (–O–) FC, (–●–) AC, (–△–) WQ and (–×–) as received.

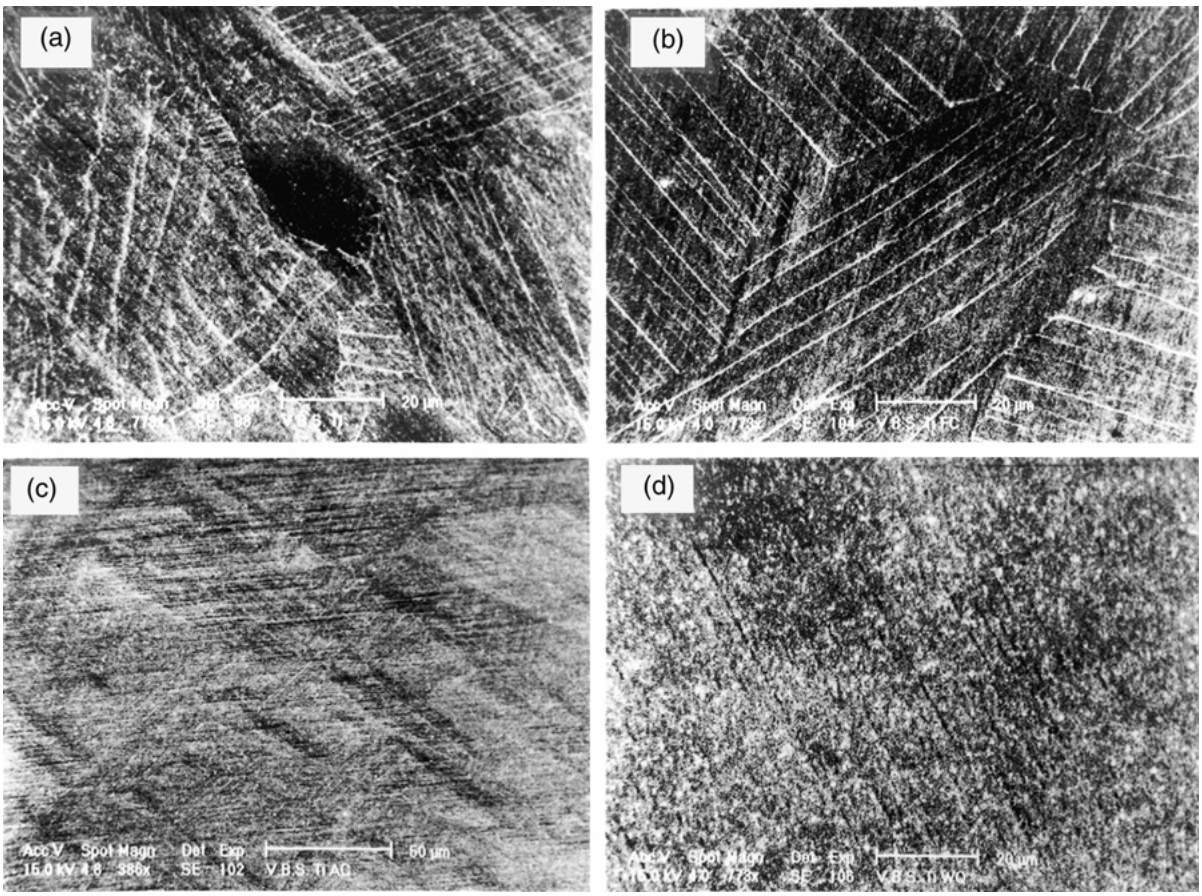

Fig. 8. SEM photomicrographs of titanium alloy (IMI 834). (a) As received (top, left), (b) FC (top, right), (c) AC (bottom, left) and (d) WQ (bottom, right).

specimens in 10.92 M phosphoric acid in ethylene glycol. The anodic polarization curves revealed active–passive behaviour for all specimens. The curves for the FC, AC and WQ specimens shifted slightly towards the lower current density region compared to those for the as received specimen. Similar anodic polarization curves for all the specimens indicated the similar anodic reactions on these surfaces.

3.4. *Structural studies: SEM and STM*

Figure 8(a) (top, left) shows the microstructure of the IMI 834 alloy (by SEM) in solution treated (1020 °C, 2 h, AC) and stabilized (700 °C, 2 h, AC) conditions. The Figure showed a duplex structure consisting of primary α (dark) and transformed β. The primary α was found to be grown at prior β grain boundaries. The microstructure after solution treatment (1080 °C, 30 min, FC, AC and WQ) are shown in Figure 8(b)–(d). The figures revealed single phase structure showing transformed β. The furnace cooled (FC) specimen (Figure 8(b), top, right) showed the retained β at the interplatelets boundaries. With increase in the cooling rate (from FC to WQ) the transformed β laths increased. The water quenched (WQ) specimen (Figure 8(d), bottom, right) showed the martensite structure.

For FC, AC and WQ specimens, after polarization studies in 7 M HCl, the α phase was preferentially attacked in the FC and AC specimens. However, in the case of the WQ specimen pitting was greater at the interplatelet boundary.

The morphology of the heat treated specimens after polarization (7 M HCl) was critically examined by STM. In general, the surface film was found to be very uniform and smooth. However, the structure of the film seemed to depend on the base structure of the heat treated alloy. The FC specimen showed rough morphology and preferential attack in the α phase and the film had a layer over layer structure (three dimensional analysis, Figure 9(a), top). The microstructural features of the film in general, are comparable and showed regular ridges and furrows appearance in the case of AC and

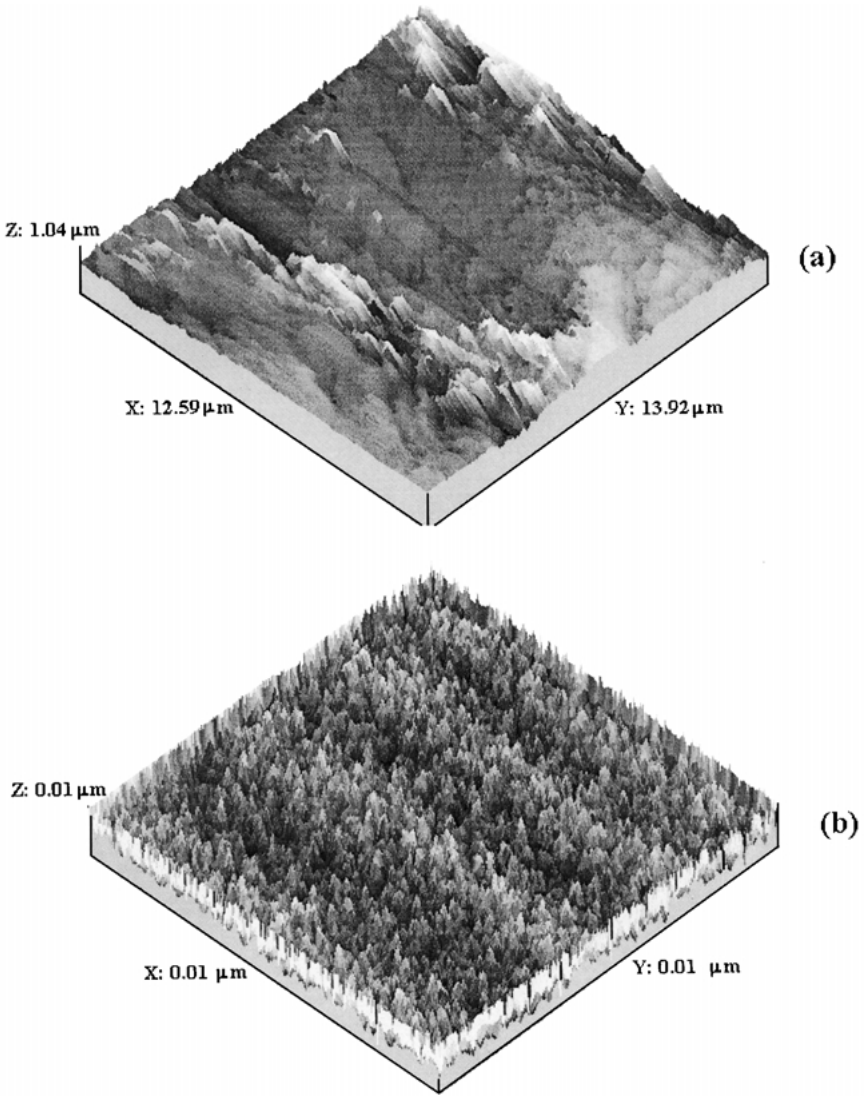

Fig. 9. STM image of titanium alloy (IMI 834) after polarization in 7 M hydrochloric acid. (a) FC and (b) AC.

WQ specimens (Figure 9(b), bottom). The furrows seem to be the result of a preferential attack on α phase by acid. The ridges are closer in the case of WQ than in AC specimen.

Acknowledgements

The authors acknowledge the Head of the Department of Chemistry at Banaras Hindu University for providing research facilities and financial assistance from CSIR, New Delhi.

References

1. E. Eylon, S. Fujishiro, P.J. Postans and F.H. Froes, *J. Met.* **1** (1984) 55–62.
2. A.A. Mazhar, F. El-Taib Heakel and A.G. Gad-Allah, *Corrosion* **44** (1988) 705.
3. S.M.A. Hosseini and V.B. Singh, *Mater. Chem. Phys.* **33** (1993) 63.
4. V.B. Singh and S.M.A. Hosseini, *Corros. Sci.* **34** (1993) 1723.
5. V.B. Singh and S.M.A. Hosseini, *Indian J. Chem. Technol.* **1** (1994) 287.
6. S.X. Yu, C.W. Brodrick, M.P. Ryan and J.R. Scully, *J. Electrochem. Soc.* **146** (1999) 4429.
7. R. Schutz, *in* D. Eylon, R. Boyer and D. Koss (Eds), 'Beta Titanium Alloys in the 1990s', (Minerals, Metals and Materials Society, Warrendale PA, 1993), p. 75.
8. P. Marcus, *Corros. Sci.* **36** (1994) 2155.
9. T. Hurlen, H. Bentzen and S. Hornkjol, *Electrochim. Acta* **32** (1987) 1613.
10. J.A. Bardwell and M.C. McKurbre, *Electrochim. Acta* **36** (1991) 647.
11. C.V.D. Alkaine, L.M.M. De Souza and F.C. Nart, *Corros. Sci.* **34** (1993) 109.
12. V.B. Singh and S.M.A. Hosseini, *J. Appl. Electrochem.* **24** (1994) 250.
13. N.T. Thomas and K. Nobe, *Corrosion* **29** (1973) 188.
14. E.J. Kelly and H.R. Bronstein, *J. Electrochem. Soc.* **131** (1984) 2232.
15. A. Caprani and J.P. Prayre, *Electrochim. Acta* **24** (1979) 835.
16. C.K. Dyer and J.S.L. Leach, *Electrochim. Acta* **23** (1978) 1387.
17. D.J. Blackwood and L.M. Peter, *Electrochim. Acta* **33** (1988) 1143.
18. P.Y. Park, E. Akiyama, H. Habazaki, A. Kawashima, K. Asami and K. Hoshimoto, *Corros. Sci.* **38** (1996) 1649.
19. X. Li, E. Akiyama, H. 1-labazaki, A. Kawashima, K. Asami and K. Hoshimoto, *Corros. Sci.* **39** (1997) 935.
20. R. Otsuka, *Sci. Papers IPRC* **54** (1960) 97.
21. R.C. May, F.H. Beck and M.G. Fontana, 'Stress Corrosion Cracking of Titanium Alloys', The Ohio State University, NGL 36-008-051 Sept. (1971).
22. T. Philips, P. Poople and L.L. Shreir, *Corros. Sci.* **12** (1972) 855.
23. A. Caprani, PhD thesis, University of Paris, CNRS A.0. **10** (1974) 1441.
24. S.H. Weiman, *Corrosion* **22** (1966) 98.
25. N.T. Thomas and K. Nobe, *J. Electrochem. Soc.* **119** (1972) 1450.
26. R.D. Armstrong and R.E. Firman, *J. Electroanal. Chem.* **34** (1979) 391.
27. J.A. Harison and D.E. Williams, *Electrochim. Acta* **27** (1982) 891.
28. L. Garfias-Mesias, M.J. Alodan, P.L. James and W.H. Smyrl, *J. Electrochem. Soc.* **145** (1998) 2005.
29. O. Bastiansen and C. Finback, 'Phosphorus and its Compounds', Vol. 1 (Interscience, New York, 1958) p. 489.
30. A.A. Mazhar, M.M. Hefny, F. El-Taib Heakel and M.S. El-Basiouny, *Brit. Corros. J.* **8** (1983) 156.
31. M. Levy, *Corrosion* **23** (1967) 236.
32. H.H. Uhlig, *Corrosion* **19** (1963) 213t.